Neuroscience 606 (2026) 31–43

Contents lists available at ScienceDirect

Neuroscience

journal homepage: www.elsevier.com/locate/nsc

Research Article

Impact of post-stroke cognitive impairment and brain connectivity on early versus late motor skill learning

Coralie van Ravestyn [a,b,c,1], Audrey Riga [a,b,c,1], Benoît Bihin [d,1], Laurence Dricot [b,1], Quentin Dessain [b,f], Nicolas Delinte [b,f], Luigi Devis [a,b], Benoît Herman [c,g], Béatrice De Coene [e], Thierry Deltombe [b,h], Jean-Marc Raymackers [i], Martin G. Edwards [c,j], Yves Vandermeeren [a,b,c,*]

[a] UCLouvain/CHU UCL Namur (Godinne), Neurology Department, Stroke Unit/Motor Learning Lab, Avenue du Dr G. Thérasse, 1, B-5530 Yvoir, Belgium
[b] UCLouvain, Institute of NeuroScience (IoNS), NEUR Division, Avenue E. Mounier, 53, B-1200 Brussels, Belgium
[c] UCLouvain, Louvain Bionics, Louvain-la-Neuve, Belgium
[d] UCLouvain, CHU UCL Namur (Godinne), Scientific Support Unit (USS), Avenue du Dr G. Thérasse, 1, B-5530 Yvoir, Belgium
[e] UCLouvain/CHU UCL Namur (Godinne), Radiology Department, Avenue du Dr G. Thérasse, 1, B-5530 Yvoir, Belgium
[f] UCLouvain, Institute of Information and Communication Technologies, Electronics and Applied Mathematics (ICTEAM), Av. Georges Lemaitre 4, 1348 Ottignies-Louvain-la-Neuve, Belgium
[g] UCLouvain, Institute of Mechanics, Materials and Civil Engineering (iMMC), Place du Levant 2, 1348 Ottignies-Louvain-la-Neuve, Belgium
[h] UCLouvain/CHU UCL Namur (Godinne), Physical Medicine and Rehabilitation Department, Avenue du Dr G. Thérasse, 1, B-5530 Yvoir, Belgium
[i] Clinique Saint-Pierre, Department of Neurology and Neurosurgery, Avenue Reine Fabiola 9, 1340 Ottignies-Louvain-la-Neuve, Belgium
[j] UCLouvain, Psychological Sciences Research Institute (IPSY), Place du Cardinal Mercier 10, 1348 Ottignies-Louvain-la-Neuve, Belgium

ARTICLE INFO

Keywords:
Stroke
Motor learning
Robotic
Cognition
Neuroimaging
Connectivity

ABSTRACT

Cognition is more engaged during early than later motor skill learning (MSkL), yet the impact of post-stroke cognitive impairment (PSCI) and brain connectivity on early MSkL remains unclear. We hypothesized that early MSkL would be impaired in people with chronic stroke compared to healthy individuals (HI), and that this impairment would be associated with PSCI, lesion burden, and structural and functional connectivity. Fifty-three people with chronic stroke and twenty-one mean age-matched HI completed a comprehensive neuropsychological assessment and trained with their contralesional/non-dominant upper limb on a speed/accuracy trade-off task across two sessions, one-week apart. Early and late MSkL were modelled and related to PSCI. To identify neural substrates and predictors of post-stroke early MSkL, multimodal brain imaging included voxel-based lesion symptom mapping, whole-brain microstructural integrity and structural–functional connectivity analyses. Both HI and people with stroke demonstrated typical MSkL patterns (retention and generalization), but HI showed steeper early MSkL. PSCI correlated with poorer early MSkL. Lesions overlapping the corticospinal tract, insula and frontal white matter tracts were associated with early MSkL deficits, while higher microstructural integrity in the posterior corpus callosum correlated with better early MSkL. Structural and functional connectome-based predictive modeling identified subcortical, temporal, visual-associative, and insular hubs with

Abbreviations: PSCI, Post-stroke cognitive impairment; MSkL, Motor skill learning; HI, Healthy individuals; UL, Upper limb; PFC, Prefrontal cortex; PPC, Posterior parietal cortex; WM, White matter; WMT, White matter tract; MRI, Magnetic resonance imaging; SD, Standard deviation; NIHSS, National Institute of Health Stroke scale; MoCA, Montreal Cognitive Assessment; RH, Right hemisphere; LH, Left hemisphere; DWI, Diffusion weighted imaging; Rs-fMRI, resting state functional MRI; TOL-F, Tower of London-version of Freiburg; MRT, Mental Rotation test; TAP, Test of attentional performance; SAT, Speed accuracy trade-off; VOI, Volume of interest; DTI, Diffusion tensor imaging; FA, Fractional anisotropy; MNI, Montreal Neurological Institute; ROI, Region of interest; PCA, Principal component analysis; PC1, First principal component; VLSM, Voxel-based lesion symptom mapping; CPM, Connectome-based predictive modelling; LOOCV, Leave-One-Out Cross-Validation; BA, Brodmann area; ACR, Anterior corona radiata; SCR, Superior corona radiata; CC, Corpus callosum; CST, Corticospinal tract; SLF, Superior longitudinal fasciculus; STG, Superior temporal gyrus; ITG, Inferior temporal gyrus; IOG, Inferior occipital gyrus; DMN, Default mode network; PLIC, Posterior limb of internal capsule; EC, External capsule.

* Corresponding author at: UCLouvain, CHU UCL Namur - Godinne, Department of Neurology, Stroke Unit / Motor Learning Lab, Avenue Dr G. Therasse, 5530 Yvoir, Belgium.
E-mail address: yves.vandermeeren@uclouvain.be (Y. Vandermeeren).

[1] CVR and AR, BB and LD contributed equally.

https://doi.org/10.1016/j.neuroscience.2026.04.018
Received 11 December 2025; Accepted 20 April 2026
Available online 21 April 2026

interhemispheric connections as key predictors of early MSkL after stroke. These findings indicate that early MSkL is selectively impaired in chronic stroke and related to PSCI and lesion burden. Multimodal neuroimaging highlighted the role of an interhemispheric network involving sensorimotor, salience, and associative regions in supporting early MSkL in chronic stroke.

Introduction

Stroke affects more than 12 million individuals worldwide each year (Feigin et al., 2025). Despite advances in acute treatment and neurorehabilitation, ~80% of stroke survivors exhibit persistent neurological impairments. These include not only motor but also post-stroke cognitive impairments (PSCI), which cover a diverse range of cognitive impairments that may selectively impact divergent cognitive functions (language, memory, attention) (Nys et al., 2007). These impairments reflect focal lesions, but also widespread disruptions of distributed brain networks supporting motor control and cognition (Grefkes and Ward, 2014; Siegel et al., 2016; Ward, 2017). Understanding how stroke lesions alter neural network connectivity and how spared circuits support recovery is central to optimizing post-stroke neurorehabilitation. Motor recovery after stroke is heterogeneous in both timing and outcome and is driven by multiple neural mechanisms (Grefkes and Ward, 2014; Hatem et al., 2016). While early improvements during the acute phase largely reflect spontaneous biological recovery processes, long-term motor recovery depends on the (re)acquisition of goal-directed motor skills through adaptive use of spared neural resources (Zeiler and Krakauer, 2013).

Motor skill learning (MSkL) is a multistage process, encompassing rapid early performance gains followed by slower improvements, retention, automatization, and generalization (Hardwick et al., 2013; Krakauer and Mazzoni, 2011; Poldrack et al., 2005; Shmuelof and Krakauer, 2011). In healthy individuals (HI), early stages of MSkL rely on cognitive processes such as attention, action planning, and performance monitoring, supported by prefrontal and parietal networks, whereas later stages become increasingly automatized and sensorimotor in nature (Doyon et al., 2003; Hardwick et al., 2018; Seidler et al., 2012; Tsay et al., 2024). This stage-dependent shift suggests that early and late phases of MSkL may be differentially vulnerable to PSCI and brain damage, yet this distinction has been insufficiently examined in the context of stroke.

After stroke, MSkL can be disrupted by direct damage to cortical or subcortical structures or by disruption of their associated white matter tracts (WMT). Successful learning often depends on compensatory recruitment of spared or atypical networks, with cognitive resources playing a particularly important role when canonical motor pathways are compromised (Mulhern, 2023; Peng et al., 2024). Although PSCI is common and clinically relevant, its contribution to specific stages of MSkL remains poorly characterized, particularly in the context of local- and network-level consequences of stroke (Forkel and Catani, 2018; Ptak and Schnider, 2010; Tsiakiri et al., 2024). It remains unclear how PSCI and distributed neural disruptions constrain early motor learning in the chronic phase of stroke.

The present study aimed to investigate how PSCI and neural damage influence early MSkL in people with chronic stroke. We hypothesized that early MSkL will be impaired relative to HI, that PSCI severity will be related to early MSkL performance, and that focal and network-level disruptions in cognitive, sensorimotor and integrative hubs will predict impaired early MSkL.

Experimental procedures

Population

Procedures were approved by the local Ethics Committee and complied with the Declaration of Helsinki. People with chronic stroke inclusion criteria were (1) supratentorial stroke (ischemic/haemorrhagic), (2) chronic phase (>6 months post-stroke) and (3) aged between 18 and 90 years. Exclusion criteria were (1) contraindications to MRI, (2) chronic use of centrally acting drugs or alcohol abuse, (3) pregnancy, (4) inability to understand, remember or execute commands due to major cognitive impairment precluding participation (determined by a phone interview with stroke people or their caregiver), (5) inability to execute commands due to major motor impairment (hemiplegia) precluding participation (determined by a phone interview), (6) uncontrolled medical conditions. For HI, the inclusion criterium was age 18–90 years; exclusion criteria were: (1) history of neurological disease, (2) drug/alcohol abuse, or (3) psychiatric disorder.

Twenty-one HI and 53 people with chronic stroke were included (July 2017-March 2019, Table 1). Age and school level were not significantly different between groups ($p = 0.09$ and 0.07, respectively). People with chronic stroke were included 31 (17–66.5) months (median (IQR)) after stroke (Fig. S1) and their overall neurological (NIHSS: 2 (0–4)) and cognitive impairments (Montreal Cognitive Assessment (MoCA): 25.5 (23.75–28)) were mild. Stroke involved the non-dominant hemisphere (i.e., controlling the non-dominant hand) of 36% of people with stroke, 21% had a haemorrhagic stroke, and 43% a strictly subcortical stroke. Twenty-three had a stroke in the right hemisphere (RH) while 30 had a stroke in the left hemisphere (LH). RH were older (RH: 65 ± 11.2 years, LH: 55.6 years ± 11.7, $p = 0.004$), but time since stroke onset was similar (RH: 51 months ± 54.3, LH: 52 ± 63.1 months, $p = 0.31$).

Study design

The research protocol took place over two weeks. Participants were evaluated two times, with one session per week (D1 and D8). People with chronic stroke first underwent a multimodal MRI session at baseline (D1) composed of 3D T1, 64 directions diffusion weighted imaging (DWI), and resting-state functional MRI (rs-fMRI) sequences. A comprehensive neuropsychological assessment was then carried out

Table 1
Demographic data of HI and people with chronic stroke. M: male, F; Female, Scholar level 1: primary education – 2: secondary education – 3: higher education, D: Dominant, ND: Non-Dominant, cx: cortical, sub-cx: subcortical, mRS: modified Rankin Scale, NIHSS: NIH Stroke Scale, MoCA: Montreal Cognitive Assessment, PHQ-9: Patient Health Questionnaire 9, Wilcoxon or Pearson test were used to test for group comparisons. Median (IQR), (%).

	HI (n = 21)	People with stroke (n = 53)	*p*
Age (years)	56 (52–62)	60 (53–70)	0.09
Sex (M/F)	12 M / 9F *(43%)*	38 M / 15F *(28%)*	
Dominant hand (R/L)	15R / 6 L *(29%)*	47R / 6 L *(11%)*	
Scholar level (1 < 2 < 3)	2 (2–3)	2 (1–2)	0.07
Time since stroke (months)		31 (17–66.5)	
Damaged hemisphere		34 D / 19 ND *(36%)*	
Localization (cortical/subcortical)		30 cx / 23 sub-cx *(43%)*	
Ischemic/Haemorrhagic		42 I / 11*H (21%)*	
mRS		1 (1–2)	
NIHSS		2 (0–4)	
MoCA		25.5 (23.75–28)	
Fazekas scale		1 (1–2)	
Depression PHQ-9	−1 (−3 – 0)	−5 (−8 – −3)	<0.001

using a range of standardized scales, which were evenly distributed over the protocol sessions, before the training on the MSkL task (Supplementary Materials). The first half of the assessment took place on D1, the second on D8.

After the neuropsychological evaluation, people with a chronic stroke were trained with their contralesional UL on a MSkL task (Fig. 1A). D1 was composed of a baseline (3 trials) followed by 20 training trials (23 trials in total), while D8 was composed of 3 retention training trials followed by 20 (continued) training trials. D8 ended with 3 generalization trials. HI followed the same experimental design, using their non-dominant UL; except that no MRI was performed and that some neuropsychological scales were not evaluated (MoCA, Tulia and Bells Test). They trained with their non-dominant UL.

Neuropsychological assessment

Cognitive functions were assessed using 17 validated neuropsychological tests (Supplementary Materials) and evaluated over D1 and D8. These tests were chosen to cover the principal cognitive functions related to motor learning (Seidler et al., 2012).

During the first session (D1), visuospatial working memory was assessed using Spatial and Arithmetical spans (Digit-$_{BACKWARDS}$ and Digit-$_{FORWARDS}$) from the WAIS-III (Tulsky et al., 2003) (good test–retest reliability and internal consistency). Visual working memory was evaluated using Corsi block tapping test (Corsi-$_{BACKWARDS}$ and Corsi-$_{FORWARDS}$) (Richardson, 2007) (adequate to good test–retest reliability and construct validity). Visual spatial attention was evaluated using the Bells' Test (Gauthier et al., 1989) (high sensitivity and good inter-rater reliability). The MoCA (Nasreddine et al., 2005) was used as a global scale to evaluate / to detect (mild) cognitive impairments (excellent sensitivity and good test–retest reliability and concurrent validity). Planning abilities were evaluated using the Tower of London digital version of Freiburg (TOL-F) (Shallice, 1982) (good construct, criterion validity and adequate reliability). Patient Health Scale 9 (PHQ-9) was used as behavioural measure of depression since depression can alter motor recovery and cognitive functions (Assadi Khalil et al., 2024; Hommel et al., 2015).

During session 2 (D8), visuospatial representation was evaluated using the Mental Rotation test (MRT) (Vandenberg and Kuse, 1978) (high internal consistency and good test–retest reliability). Various subtests of the Test of Attentional Performance (TAP) (Zimmermann and Fimm, 2002) were used to test alertness (TAP-Alertness1 and 2 and TAP-Index Alert), visual attention (TAP-Visual attention), mental flexibility (TAP-Flexibility, TAP-flex), inhibition (TAP-Go/NoGo) and working memory (TAP-Working Memory). The TAP is a standardized computerized test battery with good test–retest reliability, norm-referenced scores and established validity. Apraxia was tested using the Apraxia Screen of TULIA (Vanbellingen et al., 2010) (excellent inter-rater reliability, high sensitivity and specificity for detecting apraxia). These tests were chosen to cover the principal cognitive functions related to MSkL (Seidler et al., 2012).

Although sensorimotor impairments were not formally analysed, the selected people with stroke had a clinical diagnosis of motor impairments (clinical medical file) and the motor impairments were confirmed using phone interviews discussing difficulties in performing daily activities. The people with stroke were divided into three categories: (near-)normal use of the hand, reduced use, or non-use (plegic) hand.

Robot

The REAplan® (AXINESIS, Wavre, Belgium) is an UL endpoint robot (Baguma et al., 2020; Gilliaux et al., 2014; Riga et al., 2022), consisting of a large screen and an interactive robotic arm with a handle and forearm support allowing motion in the horizontal plane (Fig. 1B) (Fig. 1). At each session, a calibration was performed to individually adjust the height of the horizontal plane, so that the elbow was comfortably flexed at 90°. Data (X-Y positions, velocity, force exerted on the handle) were recorded at 80 Hz and stored for offline processing with custom Matlab® routines (MATLAB and Statistics Toolbox Release 2016b, The MathWorks Inc., Natick, MA, US).

Data analysis

MSkL

MSkL was assessed using the CIRCUIT task implemented on the REAplan® robot. The CIRCUIT task allowed to measure improvements of speed-accuracy trade-off (SAT), retention and generalization, as has been demonstrated in HI and people with stroke (Gerardin et al., 2022). Although formal psychometric properties such as minimal clinically important difference (MCID) have not yet been established for this task-specific robotic MSkL metric, the SAT has demonstrated construct validity, sensitivity to learning and reproducibility across multiple independent cohorts individuals and acute and chronic stroke populations (Baguma et al., 2020; Gathy et al., 2024; Gerardin et al., 2022; Riga et al., 2022).

Participants were instructed to complete as many laps as possible on a complex circuit with a cursor controlled through the robotic handle (speed constraint) while keeping the cursor within the track (accuracy

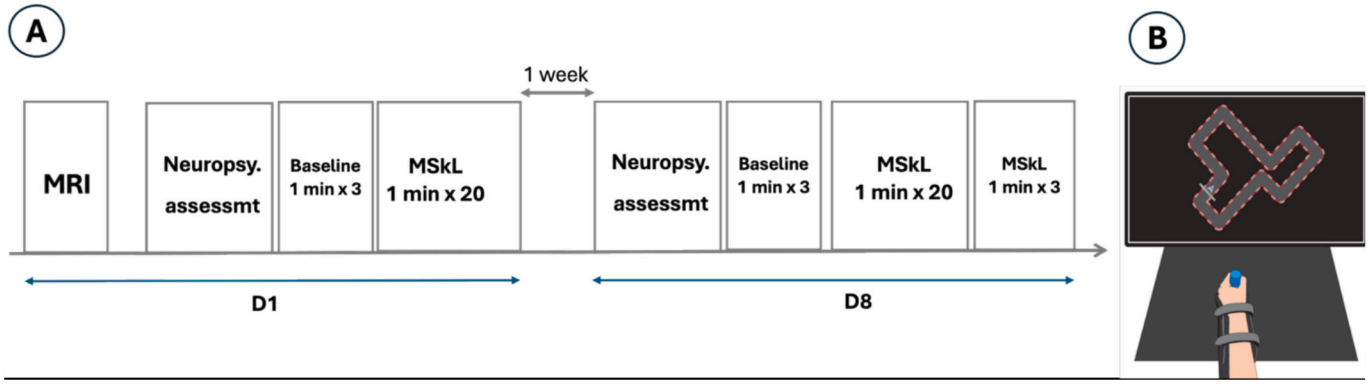

Fig. 1. Study design and robotic environment. A. Study design. On the first day (D1), people with a stroke underwent a multimodal MRI session. All participants were trained on a MSkL task (CIRCUIT) over the two sessions (D1 and D8), one week apart from each other. On D1, participants performed 3 baseline trials and then 20 training trials. On D8, 3 retention blocs were followed by 20 training trials and 3 additional generalization trials. Neuropsychological tests were administered across the two sessions (D1 and D8) before training on robot. HI did not undergo the MRI and a part of the cognitive evaluation. B. CIRCUIT task. The CIRCUIT task on the REAplan® robot was used to quantify MSkL. The participant used the handle to control the cursor and to complete as many laps as possible for 1 min while keeping the cursor within the track. MRI: Magnetic Resonance Imaging, MSkL: Motor skill learning.

constraint). On D1, after three baseline trials of 1 min, 20 training trials of 1 min were performed with the same circuit, separated by rest periods of 30 s. One week later, on D8, participants performed 3 retention trials with the same circuit to quantify D1-D8 retention, and then continued MSkL training with 20 trials on the same CIRCUIT task. Afterwards, a generalization test was performed by introducing a 90°-tilted version of the same circuit track (NEW CIRCUIT, NC) for three 1-min trials.

The speed was the cursor's velocity (cm/s) and the error was defined as the distance (cm) between the actual trajectory of the cursor and the ideal trajectory (the centre of the track). SAT was calculated in 3-s epochs, yielding 20 bins per 1-min run. The SAT was computed as follows:

$$SAT = speed/error\ (in\ arbitrary\ units,\ a.u.)$$

Baseline MSkL was defined as the performance on the first of the three baseline trials of D1 [D1T1]. Early MSkL was defined as the performance progression during the first half of training trials on D1, and was calculated as the difference between trial 12 and trial 1: [D1T12 – D1T1]. Late MSkL on D1 was defined as [D1T23 – D1T13]. One-week retention was computed as [D8T1 – D1T23], and total MSkL as [D8T23 – D1T1]. Generalization was assessed as [NCT1 – D1T1], where NCT1 refers to the first trial of the NC. The generalization drop was defined as [NCT1 – D8T23] and learning within the NC as [NCT3 – NCT1]. Our primary focus was the relationship between PSCI and early MSkL on D1 in people with chronic stroke.

MRI scanning

People with stroke were scanned on a 3 Tesla MRI scanner (Siemens Verio, Germany) with a 32-channel head coil. A 3D anatomical T1-weighted MRI (Riga et al., 2022) acquired in the sagittal plane covering the whole brain was acquired with the following parameters: field of view (FOV): 256 × 256 mm^2, matrix size: 256 × 256, slice thickness: 1 mm, pixel size: 1 mm^2, voxel size: 1 mm^3, repetition time (TR): 1600 ms, echo time (TE): 2.39 ms, flip angle (FA): 9°, number of slices: 176, no gap.

DWI was acquired with the following parameters: FOV: 256x256 mm^2, matrix size: 128x128, slice thickness: 2 mm, pixel size: 1 mm^2, voxel size: 2 mm^3, TR: 7800 ms, TE: 99 ms, 64 diffusion directions, b-value: 1000, number of slices: 50, no gap.

rs-fMRI was acquired by repeated single-shot echo-planar imaging with the following parameters: FOV: 240 × 240 mm^2, matrix size: 64 × 64, slice thickness: 3 mm, pixel size: 3 mm^2 voxel size: 3 mm^3, TR: 1800 ms, TE: 23 ms, FA: 80°, number of slices: 35, no gap (whole brain slice order ascending and interleaved). The whole brain was acquired 200 times (200 volumes).

MRI preprocessing

Lesion analysis. Using the T1 anatomical sequence, the infarcted zone (T1 positive) was manually delineated and defined as a volume of interest (VOI) under the supervision of a senior neuroradiologist. The delineation used MRIcron (Rorden et al., 2007) on the T1 volume in native space. T1 images were normalized into standard Montreal Neurological Institute stereotactic space (MNI-152) using Statistical Parametric Mapping (SPM) (Penny et al., 2007), and the native VOIs were normalized using the same parameters of normalization. Overlay maps were created, showing the extent of stroke lesions of the whole pool. Individual lesion masks were used to assess lesion volume (mm^3).

Functional MRI. rs-fMRI data were pre-processed and analyzed using BrainVoyager™ (Brain Innovation, version 23.2) (Goebel et al., 2006). A linear trend removal excluded scanner-related signal drift, temporal high-pass filter removed frequencies lower than 0.005 Hz and correction for head movements used a rigid body algorithm for rotating and translating each functional volume in 3D space. Data were corrected for time differences in acquisition of different slices. Data were co-registered with their 3D-T1 scans and normalized in the MNI space. All co-registrations were verified, and movement corrections were optimized, using a sinc interpolation. Because spontaneous low-frequency fluctuations could be contaminated by non-neural signals, additional pre-processing steps were added. Regression analyses were performed to remove artifacts due to residual motion (six movement regressors were obtained via rigid body correction of head motion implemented in BrainVoyager™) and changes in ventricles (the signal from a ventricular region of interest (ROIs) defined in each subject). The final data were smoothed in the spatial domain using a Gaussian filter, with full width at half maximum (FWHM) of 5 mm. We used BrainVoyager™ and a customized Matlab code to calculate cross-correlations between the average time-course signals extracted from 280 ROIs, intersected with each subject's individual brain mask. These regions were derived from the Brainnetome atlas (246 ROIs) (Fan et al., 2016) and the SUIT cerebellum atlas (34 ROIs) (Diedrichsen, 2006), resulting in 39,060 pairs of functional connectivity per subject.

Diffusion MRI. Elikopy pipeline (Dessain, 2024) was used to preprocess the DWI images (brain extraction (Hoopes et al., 2022), thermal denoising (Veraart et al., 2016), correction for susceptibility induced distortions, eddy-current distortion and head-motion correction (Andersson and Sotiropoulos, 2016) using FSL (v6.0.7.8) (Smith et al., 2004). The unavailability of an unweighted DWI with reversed phase-encoding led us to use Synb0-DISCO (Schilling et al., 2019) for the synthetization of a distortion-free unweighted DWI from the T1-weighted image.

Post-processing through Elikopy involved mathematical reconstruction of the DWI acquired in 64 directions to obtain the diffusion tensor imaging (DTI) mathematical model and individual DTI-derived maps of fractional anisotropy (FA) normalized in MNI space(Dessain, 2024).

Structural connectivity analysis was analyzed using the human Brainnetome atlas as for rs-fMRI data (Fan et al., 2016) which was registered using a two-step process with a Python™ implementation of the ANTS (Advanced Normalization Tools) algorithm (Avants et al., 2008) to each subject's DWI space as described above. Streamlines were generated using MRtrix3′s TCKGEN and filtered with SIFT to better match underlying fiber densities. Non-inclusive matrices were used, considering only direct tracts connecting ROI pairs, resulting in weighted 280 × 280 structural connectivity matrices for each individual. A rigid registration first aligned the DWI data to the T1 MRI subject space. Next, a non-rigid transformation was applied to align the T1 subject space with the MNI template space. The resulting transformations were applied to register the atlas ROIs to each subject's DWI space, followed by a 2-mm dilation of the ROIs to include the white–gray matter interface. Structural connectivity matrices were generated by counting the number of streamlines passing through each ROI pair, resulting in a weighted 280 × 280 connectivity matrix for each individual.

Statistical analyses

Behavioural measurements

Analyses were conducted in RStudio (version 2024.4.2.764) using R (R Foundation for Statistical Computing, 2018, Austria, Vienna, version 4.4.1).

Wilcoxon tests were used to investigate differences in neuropsychological assessment between HI and people with stroke. To summarize the neuropsychological scores into a single "global cognitive outcome" per subject within a common frame, we computed a Principal Component Analysis (PCA) using standardized scores (z-scores) from both HI and people with stroke scores. The PHQ-9 z-score was included in the PCA to account for the influence of depression PSCI (Hommel et al., 2015). For the retained cognitive scales, weights were assigned by the

PCA, indicating their contribution to the first principal component (PC1). Each participant's score on these scales was multiplied by the corresponding PC1 loading and summed to obtain an individual score representing global cognition. Exploratory post-hoc analysis was conducted to associate specific domains of cognition with early MSkL through Spearman correlations. Neuropsychological scales included in the PCA were grouped into four cognitive domains (working memory, executive functions, attention, and visuospatial processing). Composite scores were computed by averaging z-standardized test scores within each domain.

Wilcoxon tests were used to analyse the evolution of SAT at specific timepoints (Baseline, early MSkL, late MSkL, total MSkL, retention, generalization, generalization drop). Learning curves were plotted and smoothed with a loess algorithm using a span of 0.75 and a tricubic weighting to describe the kinetics of SAT over the whole protocol. Levene test was used to assess variance difference between groups. An ANCOVA model was also computed to account for baseline difference between the groups. Linear regression analyzed the relationship between global cognition and specific MSkL progressions (early and late MSkL).

Group comparisons were repeated separately for LH and RH subgroups to explore potential hemispheric differences as lesion side might influence both cognitive status and MSkL trajectories (Cano et al., 2025; Mani et al., 2013). Skewness analyses were used to rule out potential floor/ceiling effect of one of these subgroups. A multiple linear regression model was performed with early MSkL as dependant variable and global cognition, age, lesion volume, lesioned hemisphere and baseline SAT (D1T1) as predictors. Model assumptions were checked through residual diagnostics and variance inflation factors, and results are reported with regression coefficients, standard errors, p-values, and 95% confidence intervals.

Neuroimaging

Intensity histograms and cluster tables were produced for the overall lesion map and then separately for LH and RH lesion maps. Mean and SD lesion volumes were compared using a Welch two-sample *t*-test in RStudio.

VLSM was conducted using the non-parametric MRIcron toolbox (NPM, NiiStat) (Rorden et al., 2007) for associations between lesion location and early MSkL. Brunner-Munzel rank-order test was applied to voxels lesioned in at least 10% of people with stroke. Analyses were first performed on unflipped VOIs assuming asymmetrical brain organization with lesion volume as covariate. Exploratorily, analyses were repeated on flipped VOIs to increase statistical power. Statistical maps were corrected using a Freedman-Lane permutation (−3,000 permutations), with corrected threshold of $p < 0.05$. The same procedure was repeated without covariates, using normal permutations (3,000). Significant clusters were localized using MNI coordinates, MRIcroGL (Rorden and Brett, 2000), the Human Brain Atlas (Mai, 4th Ed.) (Mai et al., 2008), the BioImage Suite MNI2TAL converter (Papademetris et al., 2006), and the JHU white matter atlas (ICBM 1 mm) (Wakana et al., 2004).

To identify associations between preserved WMT integrity and early MSkL, FA maps were analyzed using ANCOVA in BrainVoyager™, with early MSkL as predictor of interest and lesion volume as covariate to control for confounding effects. A voxelwise threshold of $p < 0.0001$ was applied, with spatial smoothing (FWHM), and multiple comparison correction via Monte Carlo simulations (1,000 iterations, estimated smoothness = 5.92), leading to a minimum cluster size for significance set at 154 voxels. Significant voxels were overlaid on a WM atlas (Wakana et al., 2004) to identify corresponding tracts.

Connectome-based Predictive Modelling (CPM) was used for early MSkL prediction, separately for functional and structural connectivity (Shen et al., 2017). Connectivity matrices were computed for each participant, representing pairwise connection strengths across brain regions (ROIs). Connectivity values were used without nonlinear transformation (non-sigmoidal).

Within each training set, edges significantly correlated with early MSkL (uncorrected $p < 0.05$) were identified and split into positively and negatively correlated networks. Consistent with the original CPM framework (Shen et al., 2017), the uncorrected threshold was used at the edge-selection stage to allow the model to capture distributed network-level effects rather than relying on individually significant connections, while controlling for overfitting through cross-validation and permutation testing for each participant. Network strength was calculated by summing the weights of all retained edges within each network.

Linear regression models were then used to predict individual behavioral scores based on network strength. Covariates (age, sex, a 4-level categorical variable encoding lesion side and hand dominance, and lesion volume) were included to control for potential confounding factors. Model performance was assessed using a Leave-One-Out Cross-Validation (LOOCV) framework, in which each individual with stroke was iteratively held out as the test case (Shen et al., 2017). Importantly, at each LOOCV iteration, edge selection, network definition, network strength computation, and model fitting were performed exclusively on the training set, ensuring that no information from the held-out participant was used during model construction and thereby minimizing the risk of overfitting. Predicted scores for the left-out participant were then compared against actual behavioral values, and predictive accuracy was evaluated by fitting a regression line between predicted and observed outcomes across participants (Shen et al., 2017).

Statistical significance was assessed using permutation testing (3,000 iterations), in which behavioral labels were randomly shuffled prior to CPM model training within the same LOOCV framework, generating a null distribution of prediction accuracies against which the observed correlation was compared (Shen et al., 2017).

Bioimage Suite connectivity viewer (Papademetris et al., 2006) was used to visualize the three highest-degree nodes and most predictive edges, mapping them back onto brain anatomy to highlight network features most strongly associated with early MSkL.

Results

Neuropsychological contributors to global cognition

Group-level neuropsychological and depression scores are detailed in Table 2. The MoCA, Apraxia screen of Tulia, and Bells' Test were excluded due to limited specificity or ceiling effects. Additionally, four tests (PHQ-9, TAP Alertness 2, TAP Index Alert, and TAP Go/NoGo) were removed from the PCA (Fig. S2) as they were considered to measure a different construct (Fig. S3). The first component of the final PCA explained 40.1% of the variance and represents a "global cognitive outcome" encompassing neuropsychological functions relevant to MSkL (Seidler et al., 2012), common to both groups. Impairment in global cognition among people with chronic stroke confirmed the presence of PSCI ($F = 5.2$, $p = 0.025$, Table 2 and Table S2). The respective contributions (loadings) of individual neurocognitive scales to global cognition are detailed in Fig. S4.

Post-hoc exploratory analyses revealed significant associations between all cognitive domains and early MSkL. The strongest relationship was observed for attention ($\rho = 0.52$, $p < 0.001$), followed by executive functions ($\rho = 0.40$, $p = 0.0032$), working memory ($\rho = 0.30$, $p = 0.031$), and visuospatial processing ($\rho = 0.29$, $p = 0.036$). Although effect sizes varied across domains, all associations remained statistically significant, suggesting that multiple cognitive processes contribute to early MSkL (Table S3).

Impaired MSkL in chronic stroke

SAT trajectories were broadly similar between stroke people and HI, although people with stroke started from a lower baseline (D1T1: 6.8 ± 3.6 [a.u.] (mean ± SD) vs 9.5 ± 3.6 in HI, $t = 2.9$, $p = 0.005$; Fig. 2; Table S34; Fig. S5). Early MSkL diverged significantly between groups,

Table 2
Neuropsychological assessment. *a b c* represents the lower quartile (*a*), median (*b*), and upper quartile (*c*) for continuous variables, respectively. MoCA, Bells' test and Apraxia screen of Tulia were not assessed in HI. Wilcoxon tests were used for group comparisons. Rows highlighted in grey correspond to the 10 scales included in the final PCA, providing global cognition. TAP: Test of Attentional Performance, MoCA: Montreal Cognitive Assessment.

	HI (n = 21)	People with stroke (n = 53)	Statistic Test
Tower of London (ToL-F)	17 44 54	13 34 54	$F_{1\ 72} = 0.25$, P = 0.62
TAP-Alertness 1	14 24 34	2 10 24	$F_{1\ 72} = 8.8$, P = 0.004 *
TAP-Alertness 2	8 14 24	2 10 18	$F_{1\ 72} = 3.6$, P = 0.063
TAP-Index alert	12 18 31	10 38 73	$F_{1\ 72} = 2.5$, P = 0.12
TAP-Visual attention	38 62 66	16 62 66	$F_{1\ 72} = 0.8$, P = 0.37
TAP-Flexibility	46 79 92	7 42 73	$F_{1\ 72} = 10$, P = 0.002 *
TAP-Go/NoGo	58 58 62	34 58 62	$F_{1\ 72} = 0.12$, P = 0.73
TAP-working memory	24 38 69	7 24 46	$F_{1\ 72} = 2.5$, P = 0.12
Mental Rotation test	27 33 42	25 32 40	$F_{1\ 72} = 0.79$, P = 0.38
Digit span, forwards	6 6 7	5 6 6	$F_{1\ 72} = 7.9$, P = 0.006 *
Digit span, backwards	4 5 5	3 4 5	$F_{1\ 72} = 7.7$, P = 0.007 *
Spatial spans, forwards	5 6 6	5 6 6	$F_{1\ 72} = 0.1$, P = 0.76
Spatial spans, backwards	4 4 6	4 5 6	$F_{1\ 72} = 0.22$, P = 0.64
MoCA	/	24 26 28	
Apraxia screen of Tulia	/	11 12 12	
Bell's Test (number bells)	/	30.5 33 34	
Depression scale PHQ-9	−3 −1 0	−8 −5 −3	$F_{1\ 72} = 24$, P < 0.001 *
Global cognition	**0.11 1.0 1.62**	**−1.69 −0.43 0.85**	$\boldsymbol{F_{1\ 72} = 5.2}$, **P = 0.025** *

with HI showing steeper improvements and significantly greater gains (early MSkL: 15.7 ± 3.3 [a.u.]) than people with stroke (10.8 ± 7.3, t = 3.37, p = 0.001). People with stroke also exhibited higher variance during early MSkL (52.9 ± 7.3 a.u.) compared to late MSkL (10.9 ± 3.3, F = 4.85, p < 0.001), while HI showed similar variance across both phases (23.5 ± 4.8 vs 21.1 ± 4.6, F = 1.12, p = 0.8). Both groups displayed typical asymptotic-like learning curves with rapid early SAT improvement followed by slower gains. No significant between-group differences were observed during late MSkL (F = 0.1, p = 0.75).

Long-term retention of SAT improvement was observed between D1 and D8, despite an initial performance drop on the first block of D8 (Table S34). Introducing the NC also caused an incomplete SAT drop (i.e. with significant improvement retained compared to baseline indicating generalization), followed by rapid improvement. HI outperformed people with stroke on one-week retention, early MSkL on D8, total MSkL, and generalization drop (Table S4).

ANCOVA revealed poorer early MSkL in people with stroke compared to HI after controlling for baseline performance (β = −3.29, SE = 1.74, p < 0.001), confirming that the distinct early MSkL patterns are not solely attributable to baseline differences but reflect genuine group differences during early MSkL.

Compared to RH-damaged people with stroke, LH-damaged people with stroke showed significantly better early MSkL (F = 5.7, p = 0.021), even after adjusting for age (Est = -4.27, p = 0.042). Baseline performance did not significantly differ between groups (F = 2.1, p = 0.15), nor did late MSkL (F = 0.36, p = 0.55; Fig. S6, Table S5).

Relation between cognition and early MSkL in chronic stroke

Regression analyses in people with stroke revealed that more severe PSCI (lower global cognition scores) was associated with poorer early MSkL (r = 0.44, p = 0.001; Fig. 2), but not with late MSkL (r = 0.1, p = 0.4).

A multiple regression model indicated that better global cognition was a significant positive predictor of early MSkL (Est = 0.98; SE = 0.41, p = 0.023), and that larger lesion volume was a significant negative predictor (Est = –0.000027; SE = 0.000013; p = 0.044). Age (Est = -0.077, SE = 0.079; p = 0.33), stroke laterality (Est = 1.61, SE = 1.91; p = 0.4) and baseline performance (D1T1; p = 0.071) were not significant predictors of early MSkL. The overall model was significant (F = 6.56, p < 0.001) and explained 35% of the variance in early MSkL (adjusted R^2 = 0.35).

Standardization of predictors and outcome using z-scores revealed the number of SD change in the outcome per 1 SD increase in the predictor. Global cognition was the strongest predictor (standardized beta = 0.28, partial R^2 = 0.28), followed closely by lesion volume (standardized beta = −0.27, partial R^2 = 0.26), indicating that global cognition contributed most to the model in terms of effect size.

Voxel-based lesion symptom mapping

Due to one technical failure during MRI acquisition, imaging data were analyzed for 52 out of 53 people with stroke (29 LH and 23 RH, Fig. S7). Mean lesion volume did not significantly differ between LH and RH people with stroke: although LH stroke had a smaller mean volume (21.8 ± 36.7 mm^3), the high variance observed in RH stroke (63.3 ± 99.2 mm^3) resulted in a non-significant difference (t = -1.91, p = 0.07). This substantial disparity in volume and variance warranted its inclusion as a nuisance covariate to control for volume-related bias in voxel-wise and connectivity analyses.

VLSM did not reveal any significant cluster (BM range: z > 2.95; z (0.05) < 1.63), in either unflipped or flipped data.

The analysis was repeated without the covariate (lesion volume), revealing one significant cluster in unflipped images associated with impaired early MSkL (BM range: −1.74 < z < 3.72; z (0.05) = 3.54). This cluster encompassed the right posterior insula and external capsule (EC) and overlapped with the corticospinal tract (CST) at the level of the posterior limb of the internal capsule (PLIC) and superior corona radiata (SCR) (z = 3.57; cluster size: 154 mm^3, peak MNI coordinates: 28, −17,18; Fig. 3). In flipped images, two clusters of lesioned voxels were associated with impaired early MSkL (BM range: −3.175 < z < 4.96; z (0.05) = 3.89). The first expanded over the anterior corona radiata (ACR), superior and middle frontal gyri (cluster size: 78 mm^3, peak MNI coordinates: −21,36,15), while the second involved the supramarginal gyrus (SMG) and superior longitudinal fasciculus (SLF) (cluster size: 34 mm^3, peak MNI coordinates: −34, −24, 21) (Fig. 3).

No significant clusters were identified in relation to late MSkL.

Whole brain microstructural integrity

The analysis using whole-brain FA maps revealed a significant cluster spanning the splenium and posterior midbody of the corpus callosum (CC), where WM integrity correlated with early MSkL (2,744 mm^3, peak MNI: 4, −27, 21; r = 0.59; p < 0.0001; Fig. 4). Higher FA values–indexing better WM microstructural integrity–correlated with greater early MSkL.

Functional and structural connectivity

Using DWI and rs-fMRI within the CPM framework, we explored structural and functional connectivity patterns that predict inter-individual differences in early MSkL among people with chronic stroke.

Structural connectivity analysis included 47 of 53 people with stroke

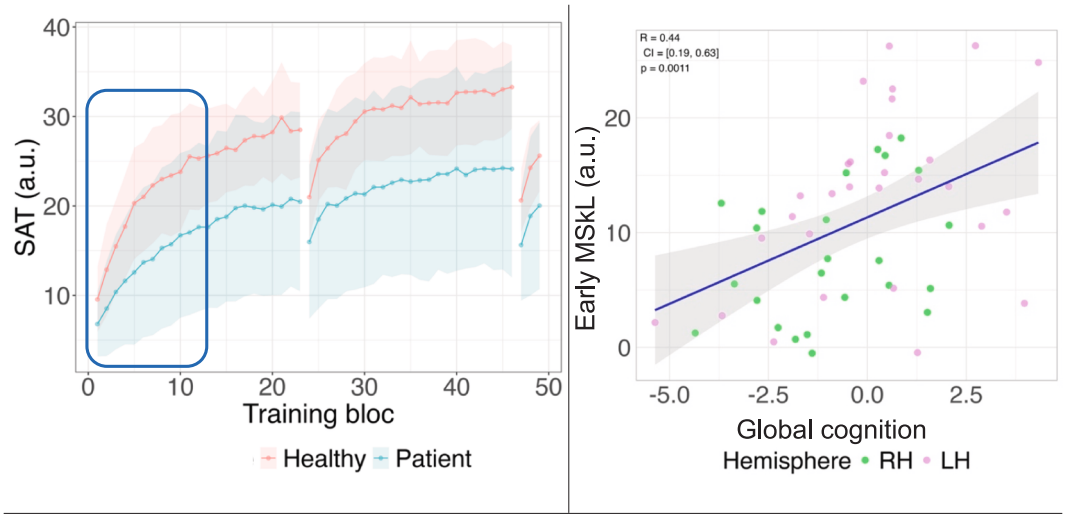

Fig. 2. MSkL in HI and people with stroke, and regression with global cognition in people with stroke. Left panel: MSkL model for HI (red) and people with stroke (blue) quantified through SAT across two sessions one week apart. The x axis represents the number of trials (23 on D1 and 23 on D8, plus 3 trials during learning with the NC). SAT is expressed in arbitrary units (a.u.). Each dot represents the group's mean SAT value for the corresponding trial; the shaded area indicates ± 1 SD. The blue box highlights early MSkL on D1 (early MSkL: 12 first trials). Right panel: Regression analysis between global cognition summarized by the global cognition score (10 cognitive tests), and early MSkL in people with chronic stroke. The regression line is shown in blue; with the grey shaded area representing the confidence interval (CI). Each dot corresponds to one individual with stroke. People with stroke in the LH and RH were separately color-coded (RH: green, LH: pink). A significant correlation was observed only for early MSkL ($r = 0.44$, $p = 0.001$). (For interpretation of the references to colour in this figure legend, the reader is referred to the web version of this article.)

(6 were excluded due to incomplete cerebellar coverage). Predicted and observed early MSkL values were significantly correlated ($r = 0.5$, $p < 0.001$) after 3,000 permutations ($p < 0.001$; Fig. S8A). The top predictive connections identified via cross-validation involved 3,208 positive and 308 negative edges (<10% of 39,060 edges defined by the atlas). Only the top 1% of nodes (n = 3 out of 280), with predictive edges spanning both hemispheres, were retained (Fig. 5, Table S6). The most predictive positive nodes were located in the right thalamus (pulvinar, degree = 60, MNI: 13,-27,8), right superior temporal gyrus (STG, Brodmann Area (BA) 22, belonging to the default mode network (DMN), degree = 43, MNI: 56,-12,-5) and left putamen (degree = 49, MNI: −17,3,-9). The same left putamen node also presented a negative edge with the left insula (BA13, MNI: −34,18,1).

Functional connectivity analysis (n = 52) also yielded significant predictions of early MSkL ($r = 0.52$, $p < 0.001$), confirmed after 3,000 permutations ($p < 0.001$, Fig. S8B). Of the 39,060 edges, 136 were positive and 922 were negative (~3%). Again, only the top 1% of nodes were analyzed (Fig. 5, Table S6), revealing key nodes with positive edges in the left inferior occipital gyrus (IOG, lingual gyrus, BA18 (visual-associative network), degree = 25, MNI: −18,-99,2) and right inferior temporal gyrus (ITG, BA20 (ventral visual-associative network), degree = 23, MNI:40,0,-43). Two nodes with negative edges were associated with poorer early MSkL: the same right ITG node and the right insula (BA13 (salience/cingulo-opercular network), degree = 28, MNI: 38,5,5; Fig. 5).

Discussion

In people with chronic stroke, early (but not late) MSkL with the contralesional UL was impaired compared to HI, and poorer early MSkL was associated with PSCI. PSCI and lesion volume emerged as key explanatory variables of early MSkL impairment in people with chronic stroke. Lesions affecting the insular-capsular, frontal and parietal regions, along with critical WMT (CST and SLF) were linked to impaired early MSkL, while microstructural integrity of the posterior CC correlated with early MSkL capacity. Both structural and functional connectivity (inter- as well as intra-hemispheric) predicted early MSkL in chronic stroke.

MSkL profiles in HI and people with stroke

HI showed rapid gains early on D1 (early MSkL), followed by shallower improvement (late MSkL), long-term retention on D8, and generalization of skill improvements. People with chronic stroke showed a similar pattern with the contralesional UL, though starting from a lower baseline and with a flatter early MSkL slope, widening the gap with HI during the early phase. Late-phase MSkL slopes became similar across groups, and people with stroke also retained performance gains over one week and showed generalization. Beyond expected overall poorer MSkL performances in people with stroke, the most pronounced difference compared to HI was observed during early MSkL.

Importantly, early MSkL gains were more variable among people with stroke, reflecting heterogeneity in PSCI profiles and lesion characteristics (Fitts, 1992; Hyndman et al., 2008; Kim et al., 2022; Tsay et al., 2024). Notably, RH stroke initially showed poorer early MSkL compared to both LH stroke and HI. However, multiple regression model showed that neither stroke laterality nor baseline SAT were predictors of early MSkL in people with stroke. Moreover, further inspection of median, interquartile range, and skewness of SAT progression revealed a symmetrically distributed range of early MSkL values in both RH and LH stroke, arguing against a floor effect (range restriction) in the RH group, supporting the analysis of the people with stroke as a single pool. Impaired early MSkL was thus a consistent feature in chronic stroke, albeit with substantial inter-individual variability, and was not influenced by stroke laterality.

PSCI, MSkL and stroke laterality

Previous findings showed that PSCI is a common consequence of stroke (El Husseini et al., 2023). Our findings are consistent with this evidence: people with chronic stroke exhibited PSCI compared to HI, as assessed using a global cognition index derived from the PCA. This approach captured the shared variance across multiple cognitive domains in both groups, providing a robust estimate of overall cognitive functioning. Past research has indicated that PCA can partially account for the individual variability in multi-domain PSCI through the reduced set of underlying behavioral dimensions (Bisogno et al., 2021; Corbetta

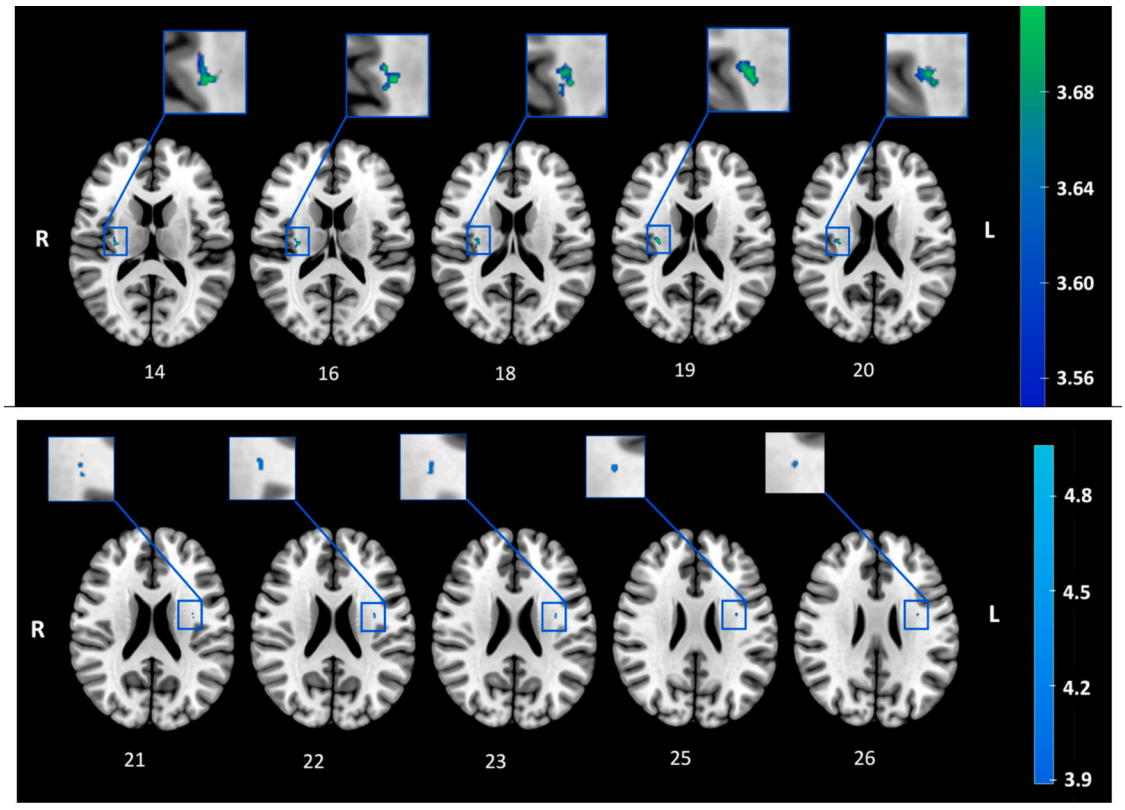

Fig. 3. VLSM of early MSkL in people with chronic stroke. Upper panel: Unflipped data. Without controlling for lesion volume, one cluster of lesioned voxels located at the bridge between the right posterior insula, EC, PLIC and SCR was associated with poor early MSkL (cluster size: 154 mm^3, peak MNI coordinates: 28, −17, 18). This cluster is displayed according to statistical significance threshold, with color shading ranging from dark blue ($z = 3.54$, $p < 0.05$, threshold corrected for 3,000 multiple permutations using the BM test) to green (highest voxel-wise BM statistic, $z = 4$). Lower panel: Data flipped to the left. Without controlling for lesion volume, two clusters of lesioned voxels were associated with poor early MSkL. The first encompassed the anterior corona radiata (ACR) and the superior and middle frontal gyri (cluster size: 78 mm^3, peak MNI coordinates: −21,36,15). The second cluster involved the supramarginal gyrus (SMG) and superior longitudinal fasciculus (SLF) (cluster size: 34 mm^3, peak MNI coordinates: −34,-24,21). Clusters are displayed according to statistical significance threshold, with color shading ranging from blue ($z = 3.89$, $p < 0.05$, corrected for 3,000 permutations using the BM test) to turquoise ($z = 4.9$, $p < 0.05$). R: right. Figure produced with MRIcroGL. (For interpretation of the references to colour in this figure legend, the reader is referred to the web version of this article.)

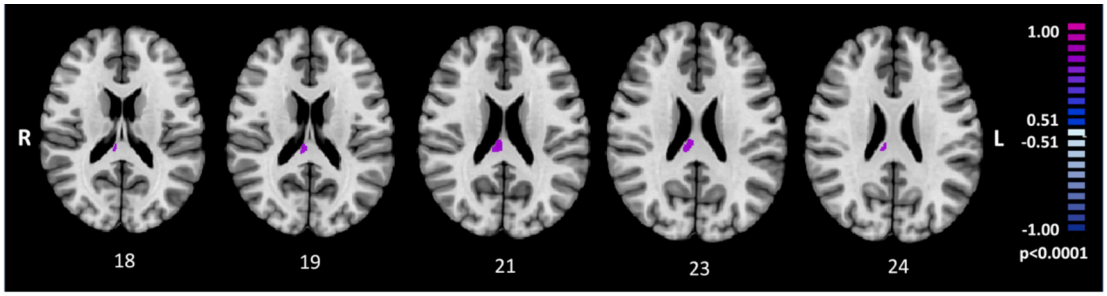

Fig. 4. Whole-brain microstructural integrity FA map related to early MSkL. One cluster was found ($r = 0.59$; $p < 0.0001$) in the corpus callosum (CC, 307 voxels, peak MNI coordinates: 4, −27, 21). Color bar represents the confidence range of F-values, with positive FA values indexing better WM microstructural integrity. R = right. Figure produced with MRIcroGL.

et al., 2015). Consistent with previous findings, the clinical reality of stroke is that individual PSCI typically spans multiple domains at once, with many people with stroke presenting with combined deficits rather than isolated impairments (Bickerton et al., 2015; Demeyere et al., 2015; Nys et al., 2007). Interestingly, a recent review outlined that up to 55% of the papers relating cognition to motor learning assessed multiple domains of cognition, such as executive functions, attention, memory (including working, visuospatial), visuospatial perception and orientation (Rajda et al., 2025). Overall, executive functions and memory (short-term, working) were the most often related to motor learning. By using a PCA-based approach, these different subdomains were summarized into a single "global cognitive outcome" common for HI and people with stroke that were related to individual MSkL performances.

PSCI, indexed by individual PCA scores, was significantly related to

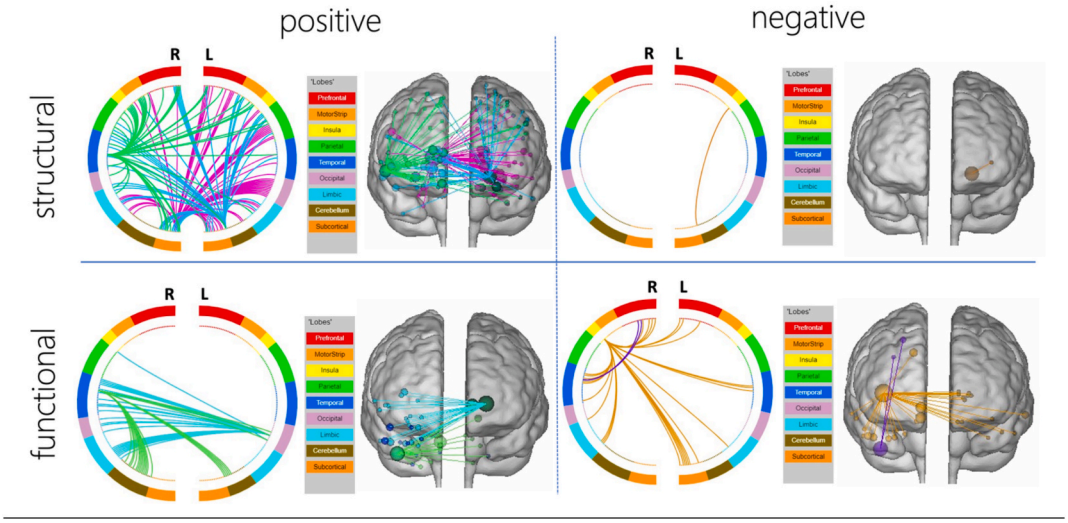

Fig. 5. Connectome-based predictive modelling (CPM). Circle and glass brain plots are displayed separately for positive (left column) and negative (right column) correlation matrices of structural (upper row) and functional connectivity (lower row). The 280x280 parcellation atlas was transformed into nine macroscale brain regions in each hemisphere. Circle plots show the connections from each of the three highest significant nodes with other regions and their specific networks. The glass brain plots provide 3D visualization of the connections between nodes through edges. For positive correlations, the three highest nodes connections are respectively displayed in pink, blue and green. For negative correlations, the connections are displayed in brown and violet. R = right, L = left. Upper row: Only the 99th percentile structural connectivity nodes (n = 3/280) were retained, containing three positive correlation nodes (top left corner: right thalamus (pulvinar, purple edges), right superior temporal gyrus (STG, BA 22, light green edges), and left putamen (light blue edges)) and a single negative correlation node (right:, same left putamen node). Lower row: 99th percentile functional connectivity nodes with two positive correlation nodes (bottom left corner: left inferior occipital gyrus (lingual gyrus, BA18, light blue edges) and right ITG (BA20, light green edges)) and two negative correlation nodes (bottom right corner: right insula (BA13, beige edges) and the same right ITG node (purple edges)). Figure produced with BioImage Suite. (For interpretation of the references to colour in this figure legend, the reader is referred to the web version of this article.)

poor early but not late MSkL in people with stroke. This pattern aligns with models proposing that early MSkL relies more heavily on attention, working memory and executive control, whereas later phases become progressively less cognitively demanding, focusing more on motor execution and ultimately leading to partial automatization (Dayan and Cohen, 2011; Seidler, 2010).

The multiple regression model further supported that PSCI and lesion volume were the primary predictors of early MSkL outcomes. Together, these findings indicate that overall cognitive functioning is an important determinant of early MSkL after stroke. The use of a global PCA-derived cognition score suggests that inter-individual differences in general cognitive capacity may influence how people with chronic stroke cope with the cognitive demands of MSkL tasks. From a clinical perspective, these results support the importance of considering overall cognitive status when delivering or designing post-stroke neurorehabilitation interventions, for example by adapting task complexity and cognitive load during early versus late learning phases.

Neural substrates of early MSkL in chronic stroke

Reflecting common stroke distribution in a general population (Karnath et al., 2018; Kernbach et al., 2023), lesions predominantly involved the middle cerebral artery territory in both hemispheres, centered on the striatum, PLIC, and SCR. However, RH stroke had more heterogeneous lesion volume and location, extending more extensively in the frontal and occipital lobes, while lesions of LH stroke were globally smaller and more centered on subcortical regions.

Grey and white matter substrates of impaired early MSkL

When controlling for lesion volume, VLSM did not reveal significant voxels associated with early MSkL, even after flipping data to increase statistical power. This lack of effect may be explained by the modest sample size (n = 52).

Exploratory analyses without lesion volume as a covariate revealed that in unflipped images, impaired early MSkL was associated with a cluster overlapping the right CST along the SCR–PLIC axis and extending to the posterior insula and EC. These findings confirm the critical role of the CST in fine motor control and MSkL and suggests additional involvement of integrative hubs and pathways such as the insula and EC in efficient early MSkL (Bloom et al., 2022; Christiansen et al.; Kerezoudis et al., 2025; Russo et al., 2021; Wang et al., 2024). In flipped data, two clusters were associated with impaired early MSkL. The first encompassed the ACR and subcortical prefrontal WM beneath the superior and middle frontal gyri, highlighting the critical role of cognitive-associative prefrontal WMT in early MSkL (Dahms et al., 2020). The second intersected the ventral branch of the SLF, SLF III (Thiebaut de Schotten et al., 2011). Prior studies emphasized the role of SLF III in the automatic capture of visual attention by salient visual targets (Thiebaut de Schotten et al., 2011). Damage to the SLF may impair early MSkL by disrupting interactions between inferior parietal, ventral premotor and ventral prefrontal regions (Janelle et al., 2022), thereby affecting motor planning, attention, execution, or sensorimotor integration (Frenkel-Toledo et al., 2019).

These findings underscore the importance of the right CST and attentional/motor-salience circuits, as well as of frontoparietal WMT such as the SLF and ACR in supporting sensorimotor integration and cognitive control during early MSkL. However, these results should be interpreted with caution, as lesion volume was not controlled for in these exploratory analyses. Therefore, the right lateralization of the CST-centered cluster might partly reflect the larger lesion sizes observed in the RH-damaged subgroup. No significant clusters were linked to late MSkL, likely due to minimal progression, supporting early MSkL as the most dynamic phase (Fig. 2).

WM microstructure analyses highlighted the posterior CC (midbody and splenium) in relation to early MSkL. Lower FA may reflect direct damage or Wallerian degeneration, indicating that reduced WM integrity in the posterior CC correlates with poorer early MSkL. Alternatively, higher FA may reflect plastic reorganization of interhemispheric WM connections, supporting better early MSkL in chronic stroke.

These posterior CC subregions support somatosensory and motor integration via interconnections between the parietal lobes (posterior midbody), and visuospatial processing via connections between the occipital and posterior temporal lobes (anterior splenium) (Musiek, 1986; Sakai et al., 2017; Tzourio-Mazoyer, 2016). This is consistent with previous work showing that callosal disruption impairs adaptive motor control (Schulz et al., 2015) and that the anterior splenium connects high-order prefrontal and temporo-parietal associative areas (Fabri and Polonara, 2023; Oliveira et al., 2022).

The CC's role in unimanual tasks reflects its importance in facilitating interhemispheric communication between motor and associative cortices (Ehrsson et al., 2000; Takeuchi et al., 2012), particularly following long-term, plastic post-stroke reconfiguration of cognitive and motor networks (Innocenti et al., 2022; Li et al., 2015; Takeuchi et al., 2012). Functional brain imaging studies showed that bilateral cortical activation is the default pattern during fine unimanual motor tasks, with callosal fibers mediating both excitatory and inhibitory interhemispheric interactions (Grefkes and Ward, 2014; Nowak et al., 2009). Damage to the CC may therefore reduce the lesioned hemisphere's ability to engage supportive contralesional networks and/or disrupt the integration of cognitive control signals critical during early MSkL.

Connectivity predictors of early MSkL

To better understand the network-level mechanisms predicting early MSkL in chronic stroke, we examined both structural and functional brain connectivity. Predictive edges spanned both inter- and intra-hemispheric networks.

CPM of structural connectivity highlights the top 1% predictive nodes, with positive edges involving the right pulvinar, left putamen and right STG (BA22), and a single negative edge between the left putamen and left insula. The pulvinar, a thalamic association nucleus, integrates cognitive, motor and sensory signals, and modulates cortical plasticity, making it a plausible hub for early MSkL (Gattass et al., 2018). Consistently, the thalamus was previously associated with MSkL in HI and acute stroke performing the CIRCUIT task (Lefebvre et al., 2012; Riga et al., 2022). Positive edges linked the right pulvinar to intrahemispheric limbic and motor regions and interhemispheric parietal and occipital regions supporting visual attention, motor translation, and cortico-subcortical loops (Casanova and Chalupa, 2023; Fama and Sullivan, 2015; Fattori et al., 2024; Krakauer, 2006).

The putamen, central to procedural and motor learning, as well as in cognitive functioning showed both positive (intra- and inter-hemispheric motor, parietal, prefrontal, and subcortical regions) and negative (left insula) edges, suggesting post-stroke reorganization could be adaptive or maladaptive. Positive edges likely support motor execution and visuospatial integration, whereas the negative edge may reflect disrupted salience-motor interactions (Menon and Uddin, 2010).

Right BA22 (STG), a multimodal association hub, connected to contralateral prefrontal, motor and parietal regions, and ipsilateral motor and subcortical regions, supports attentional, visuospatial, and motor integration (Beauchamp et al., 2004; Corbetta and Shulman, 2011). Positive edges structurally connected right BA22 with contralateral prefrontal, motor and parietal regions engaged in executive functions and reorientation of visuospatial planning (Alho et al., 2014), and with ipsilateral prefrontal, motor and subcortical regions modulating motor responses to attentional or sensory cues (Poldrack et al., 2005). The presence of interhemispheric predictive edges underscores the importance of structural integrity and adaptive reorganization beyond the lesioned hemisphere.

CPM of functional connectivity revealed positive edges in the left visual-associative cortex (BA18) and right temporal cortex (BA20), indicating visuospatial processing networks facilitate early MSkL (Seidler et al., 2012).

BA18 is a secondary visual cortex hub, linked interhemispherically to occipital, temporal, and limbic regions, reflecting the importance of cross-hemispheric visual integration for motor control (Gazzaniga et al., 2013). Its emergence as a predictive hub may reflect the need for visual-associative integration during early MSkL (Kahn et al., 2017), particularly when visual feedback is critical for motor control and refining motor strategies. Positive edges from BA18 were exclusively interhemispheric, predominantly linking occipital, temporal, and limbic regions. This suggests that efficient cross-hemispheric transfer of visual information and its integration with associative and memory-related circuits facilitates early MSkL mechanisms.

Right BA20 (ITG), is involved in higher-order cognitive functions, including object representation, decision-making, and the maintenance and retrieval of complex visual information in working memory (Lin et al., 2020), all potentially critical for early MSkL. It was predominantly connected to both the ipsi- and contralateral cerebellum via positive edges, suggesting its involvement in predictive motor control and/or error detection and correction during early MSkL (Tzvi et al., 2022). Additionally, the right ITG was linked to left occipital regions through positive interhemispheric edges, indicating that successful early MSkL may rely on coordinated visuomotor and affective-motivational integration across hemispheres (Brissenden and Somers, 2019).

Conversely, negative edges from right ITG to ipsilateral prefrontal regions may indicate inefficient reliance on executive processes. This aligns with previous findings linking disrupted functional connectivity between cortical regions with cognitive impairments, including deficits in visual information processing (Cai et al., 2023).

The right insula (BA13), a key salience network hub, emerged as a negative predictor, with widespread intra- and interhemispheric edges to prefrontal, temporal, limbic, and subcortical regions. This pattern suggests that maladaptive salience processing and disrupted network switching could hinder efficient MSkL (Manoliu et al., 2013).

To sum up, this multimodal neuroimaging approach revealed that efficient early MSkL in chronic stroke relies on diverse and widespread substrates, including visuospatial and temporal associative areas, subcortical hubs, intra- and interhemispheric WMT (ACR, SLF and CC), and interhemispheric connectivity. These findings underscore the importance of bilateral communication and integration of cognitive control, sensorimotor feedback, and procedural memory in supporting early MSkL, consistent with our behavioral observation that PSCI impairs early MSkL in chronic stroke.

Limitations

Our sample captured substantial heterogeneity in stroke characteristics (stroke location, laterality, demographics and clinical features) while excluding people with severe PSCI or hemiplegia that would have prevented task completion. Consequently, our findings primarily generalize to people with chronic stroke with mild-to-moderate motor and/or cognitive impairments.

Standardized clinical measurement of UL motor impairment (e.g., Fugl-Meyer Assessment) was not collected in this study, which limits direct comparison with conventional rehabilitation outcomes. However, motor performance and learning were objectively quantified using kinematic data (SAT), providing a sensitive and continuous measure of MSkL. Moreover, stroke people remained impaired in their capacity to achieve MSkL over time after controlling for baseline differences with HI. Our findings thus primarily generalize to individuals with mild-to-moderate motor deficits capable of executing the task. Future studies should combine robotic learning metrics with standardized clinical motor scales to bridge mechanistic and clinical perspectives.

Although RH were older than LH, time since stroke and baseline MSkL performance were comparable across groups, and age did not predict early MSkL. No significant effect of stroke laterality was noticed, and most neuropsychological scales did not differ between LH and RH.

Importantly, we chose to use PCA to derive a single global cognitive index for both HI and people with stroke. This approach allowed us to capture overall cognitive functioning within a common framework,

focusing on global impairments that are frequently observed after stroke and may influence MSkL. The cognitive tests included in the PCA were selected to cover key domains implicated in MSkL, such as attention, executive control, and visuospatial processing (Seidler et al., 2012). While the resulting global cognitive score was significantly correlated with early MSkL, the specific contributions of individual domains remain to be clarified in future studies. Specifically, the PCA-derived global cognition score should not be interpreted as implying equal weighting or equivalent relevance of all cognitive domains to motor learning; rather, it captures shared variance across interrelated processes known to support early MSkL.

RH lesions tended to be more extensive than LH lesions; however, we applied robust imaging and statistical controls (nuisance covariates, permutation-based thresholding, between-subjects factors, LOOCV) to reduce overfitting and increase reliability. Replication in a larger cohort will be important to determine whether the observed effects reflect specific regional contributions or are primarily driven by lesion volume.

Conclusion

In chronic stroke, early MSkL is impaired, contrarily to late MSkL. More severe PSCI and greater lesion burden correlated with poorer early MSkL. Multimodal brain imaging suggests that the early phase of MSkL is supported by a distributed cognitive-motor network involving salience and executive hubs, associative cortices and both intra- and inter-hemispheric connectivity.

For complex unimanual motor tasks, preserved structural and functional interhemispheric connectivity appears crucial for integrating global cognition with motor execution during early MSkL in the chronic stroke phase.

CRediT authorship contribution statement

Coralie van Ravestyn: Writing – review & editing, Writing – original draft, Visualization, Software, Methodology, Investigation, Formal analysis. **Audrey Riga:** Conceptualization, Data curation, Funding acquisition, Investigation, Methodology. **Benoît Bihin:** Formal analysis, Supervision, Validation, Visualization, Writing – review & editing. **Laurence Dricot:** Formal analysis, Software, Supervision, Validation, Visualization, Writing – review & editing. **Quentin Dessain:** Software, Formal analysis. **Nicolas Delinte:** Software, Formal analysis. **Luigi Devis:** Formal analysis, Visualization. **Benoît Herman:** Resources, Software. **Béatrice De Coene:** Supervision. **Thierry Deltombe:** Conceptualization, Investigation, Methodology. **Jean-Marc Raymackers:** Conceptualization, Investigation. **Martin G. Edwards:** Conceptualization, Investigation, Methodology, Validation, Writing – review & editing. **Yves Vandermeeren:** Writing – review & editing, Validation, Supervision, Resources, Project administration, Methodology, Investigation, Funding acquisition, Conceptualization.

Declaration of competing interest

The authors declare that they have no known competing financial interests or personal relationships that could have appeared to influence the work reported in this paper.

Acknowledgements

We are grateful to the people who participated in the study and their relatives. We thank Professor J-J Orban de Xivry (KUL) for his input during the preparation of the study. We thank Julien Sapin (AXINESIS) for help and support with the REAplan®, and Adrien Denis (UCLouvain, Louvain Bionics) for software development and implementation of the tasks.

We are grateful to the Fondation Baron Albert Frère and the Fondation Louvain that supported the implementation and development of the bimanual version of the REAplan® robot (AXINESIS, Wavre, Belgium) in the Stroke Unit of the CHU UCL Namur (site Godinne). We are grateful to the Fondation Amélie and Fondation Roi Baudouin/Fonds Amélie which support permitted to complete the study.

All procedures performed in this study were approved by the Ethics Committee of the CHU UCL Namur Mont- Godinne on December, 30 2022 (approval number: B039201421432).

Funding

The work of YV is supported by the following grants: Fonds de la Recherche Scientifique – FNRS 1.R.506.16, 1.R.506.18, 1.R.506.20F & 1.S00722F; Fonds Spécial de Recherche (FSR) from the Fédération Wallonie-Bruxelles; and Fondation Mont-Godinne.

The work of AR was supported by grants from the Fondation Mont-Godinne 2015-2016 and 2019-2020, FSR 2016-2018-2019, and Fondation Roi Baudouin/Fonds Amélie 2018-2019.

The work of CvR is supported by the following grants: FSR 2022 -2023, Fonds de la Recherche Scientifique-FRIA FC 49617 and 1. E.032.24F.

Appendix A. Supplementary data

Supplementary data to this article can be found online at https://doi.org/10.1016/j.neuroscience.2026.04.018.

Data availability

Data will be made available upon reasonable request.

References

Alho, K., Rinne, T., Herron, T.J., Woods, D.L., 2014. Stimulus-dependent activations and attention-related modulations in the auditory cortex: a meta-analysis of fMRI studies. Hear. Res. 307, 29–41. https://doi.org/10.1016/j.heares.2013.08.001.

Andersson, J.L.R., Sotiropoulos, S.N., 2016. An integrated approach to correction for off-resonance effects and subject movement in diffusion MR imaging. Neuroimage 125, 1063–1078.

Assadi Khalil, S., Kim, G.J., Rand, D., 2024. Comparison of upper extremity function and daily use in individuals with and without post stroke depression. Neurorehabil. Neural Repair 38 (2), 99–108.

Avants, B.B., Epstein, C.L., Grossman, M., Gee, J.C., 2008. Symmetric diffeomorphic image registration with cross-correlation: evaluating automated labeling of elderly and neurodegenerative brain. Med. Image Anal. 12 (1), 26–41.

Baguma, M., Yeganeh Doost, M., Riga, A., Laloux, P., Bihin, B., Vandermeeren, Y., 2020. Preserved motor skill learning in acute stroke patients. Acta Neurol. Belg. 120 (2), 365–374. https://doi.org/10.1007/s13760-020-01304-7.

Beauchamp, M.S., Lee, K.E., Argall, B.D., Martin, A., 2004. Integration of auditory and visual information about objects in superior temporal sulcus. Neuron 41 (5), 809–823. https://doi.org/10.1016/s0896-6273(04)00070-4.

Bickerton, W.L., Demeyere, N., Francis, D., Kumar, V., Remoundou, M., Balani, A., Humphreys, G.W., 2015. The BCoS cognitive profile screen: utility and predictive value for stroke. Neuropsychology 29 (4), 638–648. https://doi.org/10.1037/neu0000160.

Bisogno, A.L., Favaretto, C., Zangrossi, A., Monai, E., Facchini, S., De Pellegrin, S., Corbetta, M., 2021. A low-dimensional structure of neurological impairment in stroke. Brain Commun. 3 (2), fcab119.

Bloom, M.S., Orthmann-Murphy, J., Grinspan, J.B., 2022. Motor learning and physical exercise in adaptive myelination and remyelination. ASN Neuro 14, 17590914221097510.

Brissenden, J.A., Somers, D.C., 2019. Cortico-cerebellar networks for visual attention and working memory. Curr. Opin. Psychol. 29, 239–247.

Cai, J., Xu, M., Cai, H., Jiang, Y., Zheng, X., Sun, H., Sun, Y., 2023. Task cortical connectivity reveals different network reorganizations between mild stroke patients with cortical and subcortical lesions. Brain Sci. 13 (8).

Cano, L.A., Albarracín, A.L., Farfán, F.D., Fernández, E., 2025. Brain-hemispheric differences in the premotor area for motor planning: an approach based on corticomuscular connectivity during motor decision-making. Neuroimage 312, 121230.

Casanova, C., Chalupa, L.M., 2023. The dorsal lateral geniculate nucleus and the pulvinar as essential partners for visual cortical functions. Front. Neurosci. 17, 1258393.

Christiansen, L., Larsen, M.N., Madsen, M.J., Grey, M.J., Nielsen, J.B., Lundbye-Jensen, J., Long-term motor skill training with individually adjusted progressive difficulty enhances learning and promotes corticospinal plasticity.

Corbetta, M., Ramsey, L., Callejas, A., Baldassarre, A., Hacker, C.D., Siegel, J.S., Shulman, G.L., 2015. Common behavioral clusters and subcortical anatomy in stroke. Neuron 85 (5), 927–941.
Corbetta, M., Shulman, G.L., 2011. Spatial neglect and attention networks. Annu. Rev. Neurosci. 34, 569–599.
Dahms, C., Brodoehl, S., Witte, O.W., Klingner, C.M., 2020. The importance of different learning stages for motor sequence learning after stroke. Hum. Brain Mapp. 41 (1), 270–286.
Dayan, E., Cohen, L.G., 2011. Neuroplasticity subserving motor skill learning. Neuron 72 (3), 443–454. https://doi.org/10.1016/j.neuron.2011.10.008S0896-6273(11)00918-4.
Demeyere, N., Riddoch, M.J., Slavkova, E.D., Bickerton, W.L., Humphreys, G.W., 2015. The oxford cognitive screen (OCS): validation of a stroke-specific short cognitive screening tool. Psychol. Assess. 27 (3), 883–894. https://doi.org/10.1037/pas0000082.
Dessain, Q., Mathieu, S., Delinte, N., 2024. Hyedryn/elikopy:v0.3-bug fixes (v0.3).
Diedrichsen, J., 2006. A spatially unbiased atlas template of the human cerebellum. Neuroimage 33 (1), 127–138. https://doi.org/10.1016/j.neuroimage.2006.05.056.
Doyon, J., Penhune, V., Ungerleider, L.G., 2003. Distinct contribution of the cortico-striatal and cortico-cerebellar systems to motor skill learning. Neuropsychologia 41 (3), 252–262. https://doi.org/10.1016/s0028-3932(02)00158-6.
Ehrsson, H.H., Fagergren, A., Jonsson, T., Westling, G., Johansson, R.S., Forssberg, H., 2000. Cortical activity in precision- versus power-grip tasks: an fMRI study. J. Neurophysiol. 83 (1), 528–536. https://doi.org/10.1152/jn.2000.83.1.528.
El Husseini, N., Katzan, I.L., Rost, N.S., Blake, M.L., Byun, E., Pendlebury, S.T., Smith, E. E., 2023. Cognitive impairment after ischemic and hemorrhagic stroke: a scientific statement from the American Heart Association/American Stroke Association. Stroke 54 (6), e272–e291. https://doi.org/10.1161/str.0000000000000430.
Fabri, M., Polonara, G., 2023. Functional topography of the corpus callosum as revealed by fMRI and behavioural studies of control subjects and patients with callosal resection. Neuropsychologia 183, 108533. https://doi.org/10.1016/j.neuropsychologia.2023.108533.
Fama, R., Sullivan, E.V., 2015. Thalamic structures and associated cognitive functions: relations with age and aging. Neurosci. Biobehav. Rev. 54, 29–37.
Fan, L., Li, H., Zhuo, J., Zhang, Y., Wang, J., Chen, L., Jiang, T., 2016. The human brainnetome atlas: a new brain atlas based on connectional architecture. Cereb. Cortex 26 (8), 3508–3526.
Fattori, P., De Vitis, M., Filippini, M., Vaccari, F.E., Diomedi, S., Gamberini, M., Galletti, C., 2024. Visual sensitivity at the service of action control in posterior parietal cortex. Front. Physiol. 15, 1408010.
Feigin, V.L., Brainin, M., Norrving, B., Martins, S.O., Pandian, J., Lindsay, P., Rautalin, I., 2025. World stroke organization: global stroke fact sheet 2025. Int. J. Stroke 20 (2), 132–144. https://doi.org/10.1177/17474930241308142.
Fitts, P.M., 1992. The information capacity of the human motor system in controlling the amplitude of movement. 1954. J. Exp. Psychol. Gen., 121(3), 262-269. doi: 10.1037//0096-3445.121.3.262.
Forkel, S.J., Catani, M., 2018. Lesion mapping in acute stroke aphasia and its implications for recovery. Neuropsychologia 115, 88–100. https://doi.org/10.1016/j.neuropsychologia.2018.03.036.
Frenkel-Toledo, S., Fridberg, G., Ofir, S., Bartur, G., Lowenthal-Raz, J., Granot, O., Soroker, N., 2019. Lesion location impact on functional recovery of the hemiparetic upper limb. PLoS One 14 (7), e0219738. https://doi.org/10.1371/journal.pone.0219738.
Gathy, E., Cadiat, N., Gerardin, E., Lambert, J., Herman, B., Leeuwerck, M., Vandermeeren, Y., 2024. Bimanual coordinated motor skill learning in patients with a chronic cerebellar stroke. Exp. Brain Res. 242 (6), 1517–1531. https://doi.org/10.1007/s00221-024-06830-x.
Gattass, R., Soares, J., Lima, B., 2018. The role of the pulvinar in spatial visual attention. In (Vol. 225, pp. 57-60).
Gauthier, L., Dehaut, F., Joanette, Y., 1989. The Bells Test: a quantitative and qualitative test for visual neglect. Int. J. Clin. Neuropsychol. 11 (2), 49–54.
Gazzaniga, M., Ivry, R., Mangun, G., 2013. Cognitive neuroscience-the biology of the mind (W. W. Norton & Company Ed. Fourth ed.).
Gerardin, E., Bontemps, D., Babuin, N.T., Herman, B., Denis, A., Bihin, B., Vandermeeren, Y., 2022. Bimanual motor skill learning with robotics in chronic stroke: comparison between minimally impaired and moderately impaired patients, and healthy individuals. J. Neuroeng. Rehabil. 19 (1), 28. https://doi.org/10.1186/s12984-022-01009-3.
Gilliaux, M., Lejeune, T.M., Detrembleur, C., Sapin, J., Dehez, B., Selves, C., Stoquart, G., 2014. Using the robotic device REAplan as a valid, reliable, and sensitive tool to quantify upper limb impairments in stroke patients. J Rehabil Med 46 (2), 117–125. https://doi.org/10.2340/16501977-1245.
Goebel, R., Esposito, F., Formisano, E., 2006. Analysis of functional image analysis contest (FIAC) data with brainvoyager QX: from single-subject to cortically aligned group general linear model analysis and self-organizing group independent component analysis. Hum. Brain Mapp. 27 (5), 392–401.
Grefkes, C., Ward, N.S., 2014. Cortical reorganization after stroke: how much and how functional? Neuroscientist 20 (1), 56–70. https://doi.org/10.1177/1073858413491147.
Hardwick, R.M., Caspers, S., Eickhoff, S.B., Swinnen, S.P., 2018. Neural correlates of action: comparing meta-analyses of imagery, observation, and execution. Neurosci. Biobehav. Rev. 94, 31–44. https://doi.org/10.1016/j.neubiorev.2018.08.003.
Hardwick, R.M., Rottschy, C., Miall, R.C., Eickhoff, S.B., 2013. A quantitative meta-analysis and review of motor learning in the human brain. Neuroimage 67, 283–297. https://doi.org/10.1016/j.neuroimage.2012.11.020.
Hatem, S.M., Saussez, G., Della Faille, M., Prist, V., Zhang, X., Dispa, D., Bleyenheuft, Y., 2016. Rehabilitation of motor function after stroke: a multiple systematic review focused on techniques to stimulate upper extremity recovery. Front. Hum. Neurosci. 10, 442. https://doi.org/10.3389/fnhum.2016.00442.
Hommel, M., Carey, L., Jaillard, A., 2015. Depression: cognition relations after stroke. Int. J. Stroke 10 (6), 893–896. https://doi.org/10.1111/ijs.12057.
Hoopes, A., Mora, J.S., Dalca, A.V., Fischl, B., Hoffmann, M., 2022. SynthStrip: skull-stripping for any brain image. Neuroimage 260, 119474.
Hyndman, D., Pickering, R.M., Ashburn, A., 2008. The influence of attention deficits on functional recovery post stroke during the first 12 months after discharge from hospital. J. Neurol. Neurosurg. Psychiatry 79 (6), 656–663. https://doi.org/10.1136/jnnp.2007.125609.
Innocenti, G.M., Schmidt, K., Milleret, C., Fabri, M., Knyazeva, M.G., Battaglia-Mayer, A., Caminiti, R., 2022. The functional characterization of callosal connections. Prog. Neurobiol. 208, 102186.
Janelle, F., Iorio-Morin, C., D'Amour, S., Fortin, D., 2022. Superior longitudinal fasciculus: a review of the anatomical descriptions with functional correlates. Front. Neurol. 13, 794618.
Kahn, A.E., Mattar, M.G., Vettel, J.M., Wymbs, N.F., Grafton, S.T., Bassett, D.S., 2017. Structural pathways supporting swift acquisition of new visuomotor skills. Cereb. Cortex 27 (1), 173–184.
Karnath, H.O., Sperber, C., Rorden, C., 2018. Mapping human brain lesions and their functional consequences. Neuroimage 165, 180–189.
Kerezoudis, P., Jensen, M.A., Klassen, B.T., Worrell, G.A., Gregg, N.M., Ince, N.F., Miller, K.J., 2025. The human insula encodes somatotopic representation of motor execution with an effector-specific connectomic map to primary motor cortex. bioRxiv.
Kernbach, J.M., Hartwigsen, G., Lim, J.S., Bae, H.J., Yu, K.H., Schlaug, G., Bzdok, D., 2023. Bayesian stroke modeling details sex biases in the white matter substrates of aphasia. Commun. Biol. 6 (1), 354.
Kim, J., Cha, B., Lee, D., Kim, J.M., Kim, M., 2022. Effect of cognition recovery by repetitive transcranial magnetic stimulation on ipsilesional dorsolateral prefrontal cortex in subacute stroke patients. Front. Neurol. 13, 823108.
Krakauer, J.W., 2006. Motor learning: its relevance to stroke recovery and neurorehabilitation. Curr. Opin. Neurol. 19 (1), 84–90. https://doi.org/10.1097/01.wco.0000200544.29915.cc.
Krakauer, J.W., Mazzoni, P., 2011. Human sensorimotor learning: adaptation, skill, and beyond. Curr. Opin. Neurobiol. 21 (4), 636–644. https://doi.org/10.1016/j.conb.2011.06.012S0959-4388(11)00121-8.
Lefebvre, S., Dricot, L., Gradkowski, W., Laloux, P., Vandermeeren, Y., 2012. Brain activations underlying different patterns of performance improvement during early motor skill learning. Neuroimage 62 (1), 290–299. https://doi.org/10.1016/j.neuroimage.2012.04.052.
Li, Y., Wu, P., Liang, F., Huang, W., 2015. The microstructural status of the corpus callosum is associated with the degree of motor function and neurological deficit in stroke patients. PLoS One 10 (4), e0122615.
Lin, Y.H., Young, I.M., Conner, A.K., Glenn, C.A., Chakraborty, A.R., Nix, C.E., Sughrue, M.E., 2020. Anatomy and white matter connections of the inferior temporal gyrus. World Neurosurg. 143, e656–e666. https://doi.org/10.1016/j.wneu.2020.08.058.
Mai, J.K., Paxinos, G., Voss, T., 2008. Atlas of the human brain. Elsevier Science.
Mani, S., Mutha, P.K., Przybyla, A., Haaland, K.Y., Good, D.C., Sainburg, R.L., 2013. Contralesional motor deficits after unilateral stroke reflect hemisphere-specific control mechanisms. Brain 136 (Pt 4), 1288–1303.
Manoliu, A., Meng, C., Brandl, F., Doll, A., Tahmasian, M., Scherr, M., Sorg, C., 2013. Insular dysfunction within the salience network is associated with severity of symptoms and aberrant inter-network connectivity in major depressive disorder. Front. Hum. Neurosci. 7, 930.
Menon, V., Uddin, L.Q., 2010. Saliency, switching, attention and control: a network model of insula function. Brain Struct. Funct. 214 (5–6), 655–667.
Mulhern, M., 2023. Cognitive rehabilitation interventions for post-stroke populations. Dela J. Public Health 9 (3), 70–74. https://doi.org/10.32481/djph.2023.08.012.
Musiek, F.E., 1986. Neuroanatomy, neurophysiology, and central auditory assessment. Part III: corpus callosum and efferent pathways. Ear Hear. 7 (6), 349–358. https://doi.org/10.1097/00003446-198612000-00001.
Nasreddine, Z.S., Phillips, N.A., Bédirian, V., Charbonneau, S., Whitehead, V., Collin, I., Chertkow, H., 2005. The montreal cognitive assessment, MoCA: a brief screening tool for mild cognitive impairment. J. Am. Geriatr. Soc. 53 (4), 695–699. https://doi.org/10.1111/j.1532-5415.2005.53221.x.
Nowak, D.A., Grefkes, C., Ameli, M., Fink, G.R., 2009. Interhemispheric competition after stroke: brain stimulation to enhance recovery of function of the affected hand. Neurorehabil. Neural Repair 23 (7), 641–656. https://doi.org/10.1177/1545968309336661.
Nys, G.M., van Zandvoort, M.J., de Kort, P.L., Jansen, B.P., de Haan, E.H., Kappelle, L.J., 2007. Cognitive disorders in acute stroke: prevalence and clinical determinants. Cerebrovasc. Dis. 23 (5–6), 408–416. https://doi.org/10.1159/000101464.
Oliveira, R., Pelentritou, A., Di Domenicantonio, G., De Lucia, M., Lutti, A., 2022. In vivo estimation of axonal morphology from magnetic resonance imaging and electroencephalography data. Front. Neurosci. 16, 874023.
Papademetris, X., Jackowski, M.P., Rajeevan, N., DiStasio, M., Okuda, H., Constable, R. T., Staib, L.H., 2006. BioImage suite: an integrated medical image analysis suite: an update. Insight J. 2006, 209.
Peng, X., Srivastava, S., Sutton, F., Zhang, Y., Badran, B.W., Kautz, S.A., 2024. Compensatory increase in ipsilesional supplementary motor area and premotor connectivity is associated with greater gait impairments: a personalized fMRI

analysis in chronic stroke. Front. Hum. Neurosci. 18, 1340374. https://doi.org/10.3389/fnhum.2024.1340374.
Penny, W., Friston, K., Ashburner, J., Kiebel, S., Nichols, T., 2007. Statistical parametric mapping: the analysis of functional brain images.
Poldrack, R.A., Sabb, F.W., Foerde, K., Tom, S.M., Asarnow, R.F., Bookheimer, S.Y., Knowlton, B.J., 2005. The neural correlates of motor skill automaticity. J. Neurosci. 25 (22), 5356–5364.
Ptak, R., Schnider, A., 2010. The dorsal attention network mediates orienting toward behaviorally relevant stimuli in spatial neglect. J. Neurosci. 30 (38), 12557–12565.
Rajda, C.M., Desabrais, K., Levin, M.F., 2025. Relationships between cognitive impairments and motor learning after stroke: a scoping review. Neurorehabil. Neural Repair 39 (2), 142–156.
Richardson, J.T.E., 2007. Measures of short-term memory: a historical review. Cortex 43 (5), 635–650. https://doi.org/10.1016/S0010-9452(08)70493-3.
Riga, A., Gathy, E., Ghinet, M., De Laet, C., Bihin, B., Regnier, M., Vandermeeren, Y., 2022. Evidence of motor skill learning in acute stroke patients without lesions to the thalamus and internal capsule. Stroke 53 (7), 2361–2368.
Rorden, C., Brett, M., 2000. Stereotaxic display of brain lesions. Behav. Neurol. 12 (4), 191–200. https://doi.org/10.1155/2000/421719.
Rorden, C., Karnath, H.O., Bonilha, L., 2007. Improving lesion-symptom mapping. J. Cogn. Neurosci. 19 (7), 1081–1088. https://doi.org/10.1162/jocn.2007.19.7.1081.
Russo, C., Veronelli, L., Casati, C., Monti, A., Perucca, L., Ferraro, F., Bolognini, N., 2021. Explicit motor sequence learning after stroke: a neuropsychological study. Exp. Brain Res. 239 (7), 2303–2316.
Sakai, T., Mikami, A., Suzuki, J., Miyabe-Nishiwaki, T., Matsui, M., Tomonaga, M., Oishi, K., 2017. Developmental trajectory of the corpus callosum from infancy to the juvenile stage: comparative MRI between chimpanzees and humans. PLoS One 12 (6), e0179624.
Schilling, K.G., Blaber, J., Huo, Y., Newton, A., Hansen, C., Nath, V., Landman, B.A., 2019. Synthesized b0 for diffusion distortion correction (Synb0-DisCo). Magn. Reson. Imaging 64, 62–70.
Schulz, R., Braass, H., Liuzzi, G., Hoerniss, V., Lechner, P., Gerloff, C., Hummel, F.C., 2015. White matter integrity of premotor-motor connections is associated with motor output in chronic stroke patients. Neuroimage Clin. 7, 82–86. https://doi.org/10.1016/j.nicl.2014.11.006.
Seidler, R.D., 2010. Neural correlates of motor learning, transfer of learning, and learning to learn. Exerc. Sport Sci. Rev. 38 (1), 3–9.
Seidler, R.D., Bo, J., Anguera, J.A., 2012. Neurocognitive contributions to motor skill learning: the role of working memory. J. Mot. Behav. 44 (6), 445–453. https://doi.org/10.1080/00222895.2012.672348.
Shallice, T., 1982. Specific impairments of planning. Philos. Trans. R. Soc. Lond. B Biol. Sci. 298 (1089), 199–209. https://doi.org/10.1098/rstb.1982.0082.
Shen, X., Finn, E.S., Scheinost, D., Rosenberg, M.D., Chun, M.M., Papademetris, X., Constable, R.T., 2017. Using connectome-based predictive modeling to predict individual behavior from brain connectivity. Nat. Protoc. 12 (3), 506–518.
Shmuelof, L., Krakauer, J.W., 2011. Are we ready for a natural history of motor learning? Neuron 72 (3), 469–476. https://doi.org/10.1016/j.neuron.2011.10.017S0896-6273(11)00929-9.
Siegel, J.S., Ramsey, L.E., Snyder, A.Z., Metcalf, N.V., Chacko, R.V., Weinberger, K., Corbetta, M., 2016. Disruptions of network connectivity predict impairment in multiple behavioral domains after stroke. PNAS 113 (30), E4367–E4376. https://doi.org/10.1073/pnas.1521083113.
Smith, S.M., Jenkinson, M., Woolrich, M.W., Beckmann, C.F., Behrens, T.E., Johansen-Berg, H., Matthews, P.M., 2004. Advances in functional and structural MR image analysis and implementation as FSL. Neuroimage 23 (Suppl 1), S208–S219. https://doi.org/10.1016/j.neuroimage.2004.07.051.
Takeuchi, N., Oouchida, Y., Izumi, S., 2012. Motor control and neural plasticity through interhemispheric interactions. Neural Plast. 2012, 823285.
Thiebaut de Schotten, M., Dell'Acqua, F., Forkel, S.J., Simmons, A., Vergani, F., Murphy, D.G., Catani, M., 2011. A lateralized brain network for visuospatial attention. Nat. Neurosci. 14 (10), 1245–1246. https://doi.org/10.1038/nn.2905.
Tsay, J.S., Kim, H.E., McDougle, S.D., Taylor, J.A., Haith, A., Avraham, G., Ivry, R.B., 2024. Fundamental processes in sensorimotor learning: reasoning, refinement, and retrieval. Elife 13. https://doi.org/10.7554/eLife.91839.
Tsiakiri, A., Giantsios, C., Vlotinou, P., Nikolaidou, A., Atanbori, J., Sohani, B., Frantzidis, C., 2024. Mapping brain networks and cognitive functioning after stroke: a systematic review. Brain Organoid Syst. Neurosci. J. 2, 43–52. https://doi.org/10.1016/j.bosn.2024.08.001.
Tulsky, D.S., Chiaravalloti, N.D., Palmer, B.W., Chelune, G.J., 2003. Chapter 3 - the wechsler memory scale, third edition: a new perspective. In: Tulsky, D.S., Saklofske, D.H., Heaton, R.K., Bornstein, R., Ledbetter, M.F., Chelune, G.J., Ivnik, R. J., Prifitera, A. (Eds.), Clinical Interpretation of the WAIS-III and WMS-III. Academic Press, San Diego, pp. 93–139.
Tzourio-Mazoyer, N., 2016. Intra- and inter-hemispheric connectivity supporting hemispheric specialization. In Kennedy, H., Van Essen, D.C., Christen, Y. (Eds.), Micro-, Meso- and Macro-Connectomics of the Brain (pp. 129-146). Cham CH: 2016, The Author(s).
Tzvi, E., Loens, S., Donchin, O., 2022. Mini-review: the role of the cerebellum in visuomotor adaptation. Cerebellum 21 (2), 306–313.
Vanbellingen, T., Kersten, B., Van Hemelrijk, B., Van de Winckel, A., Bertschi, M., Müri, R., Bohlhalter, S., 2010. Comprehensive assessment of gesture production: a new test of upper limb apraxia (TULIA). Eur. J. Neurol. 17 (1), 59–66. https://doi.org/10.1111/j.1468-1331.2009.02741.x.
Vandenberg, S.G., Kuse, A.R., 1978. Mental rotations, a group test of three-dimensional spatial visualization. Percept. Mot. Skills 47 (2), 599–604. https://doi.org/10.2466/pms.1978.47.2.599.
Veraart, J., Novikov, D.S., Christiaens, D., Ades-Aron, B., Sijbers, J., Fieremans, E., 2016. Denoising of diffusion MRI using random matrix theory. Neuroimage 142, 394–406.
Wakana, S., Jiang, H., Nagae-Poetscher, L.M., van Zijl, P.C., Mori, S., 2004. Fiber tract-based atlas of human white matter anatomy. Radiology 230 (1), 77–87. https://doi.org/10.1148/radiol.2301021640.
Wang, C., Yu, Y., Yang, J., 2024. Contributions of the primary sensorimotor cortex and posterior parietal cortex to motor learning and transfer. Brain Sci. 14 (12).
Ward, N.S., 2017. Restoring brain function after stroke - bridging the gap between animals and humans. Nat. Rev. Neurol. 13 (4), 244–255. https://doi.org/10.1038/nrneurol.2017.34.
Zeiler, S.R., Krakauer, J.W., 2013. The interaction between training and plasticity in the poststroke brain. Curr. Opin. Neurol. 26 (6), 609–616. https://doi.org/10.1097/wco.0000000000000025.
Zimmermann, P., Fimm, B., 2002. A test battery for attentional performance. Applied neuropsychology of attention: theory. Diagnosis Rehabilit., 110-151.